

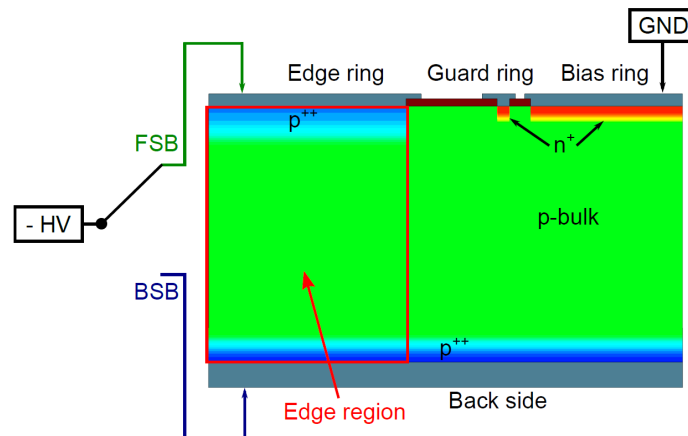
Front-side biasing of n-in-p silicon strip detectors

Marta Baselga^a, Thomas Bergauer^b, Alexander Dierlamm^a, Marko Dragicevic^b, Axel König^b, Marius Metzler^a, Elias Pree^b

a) KIT b) HEPHY

INSTITUT FÜR EXPERIMENTELLE TEILCHENPHYSIK

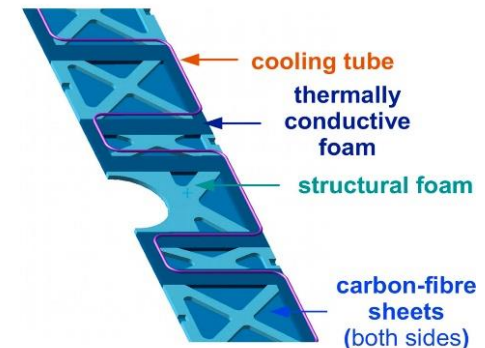
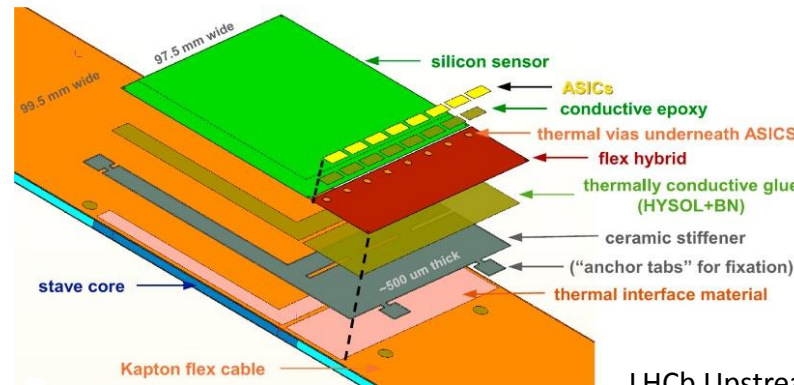
32nd RD50 Workshop
in Hamburg



Why front-side biasing?

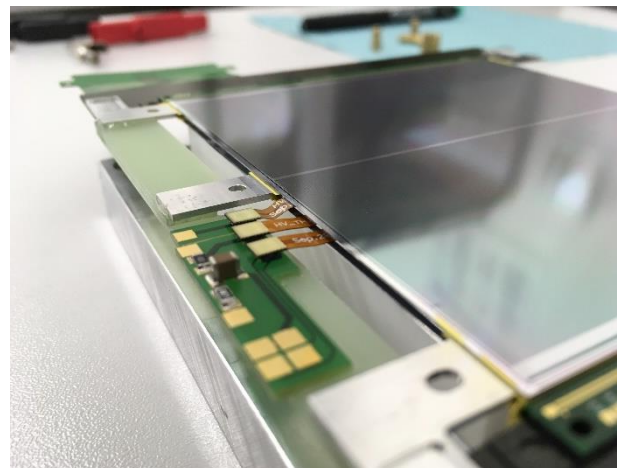
- Module assembly could be simplified by accessing front-side only
 - connecting back-side for biasing sometimes tricky

Passivated back-side



LHCb Upstream Tracker, *NIM A831 (2016) 367–369*

Sandwich structures



CMS OT proto. module

Disclaimer

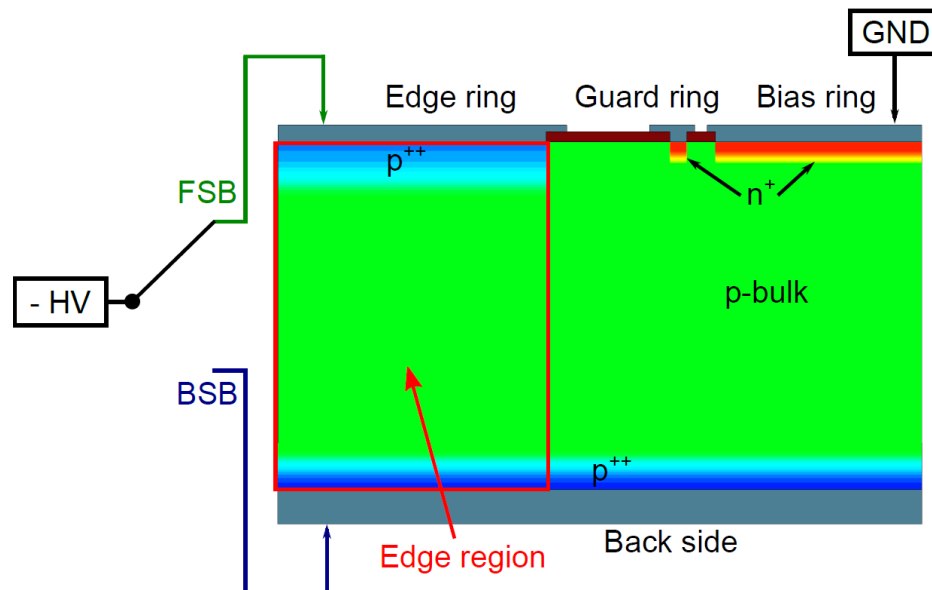
- This study focuses on the applicability in large scale systems, for which also a simplified assembly is required
- Most of the previous studies on this subject concentrated on n-type silicon; here we investigate p-type material!
- Study how FSB is influenced by:
 - operation temperature
 - irradiation
 - annealing

Edge view

- While bias ring is on ground either back-side (BSB) or front-side (FSB) could be connected to HV
- Edge region forms a p^{++} - p - p^{++} contact and is initially conductive
 - resistivity is defined by the bulk and the resistance of the contact to the back-side is defined by the geometry

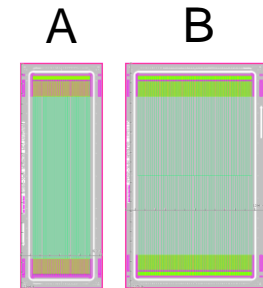
$$R_{\text{edge}} = \rho_{\text{edge}} \cdot D / A_{\text{edge}}$$

- problems arise when bulk resistivity increases...

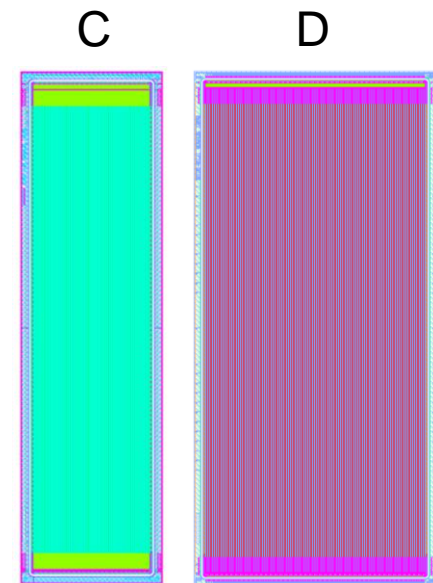


Samples

- n⁺⁺-p mini-sensors of two vendors (HPK, IFX)
 - most of earlier studies concentrated on n-type material
- Different thicknesses (mainly ddFZ indicated in name)
- Different sensor geometries



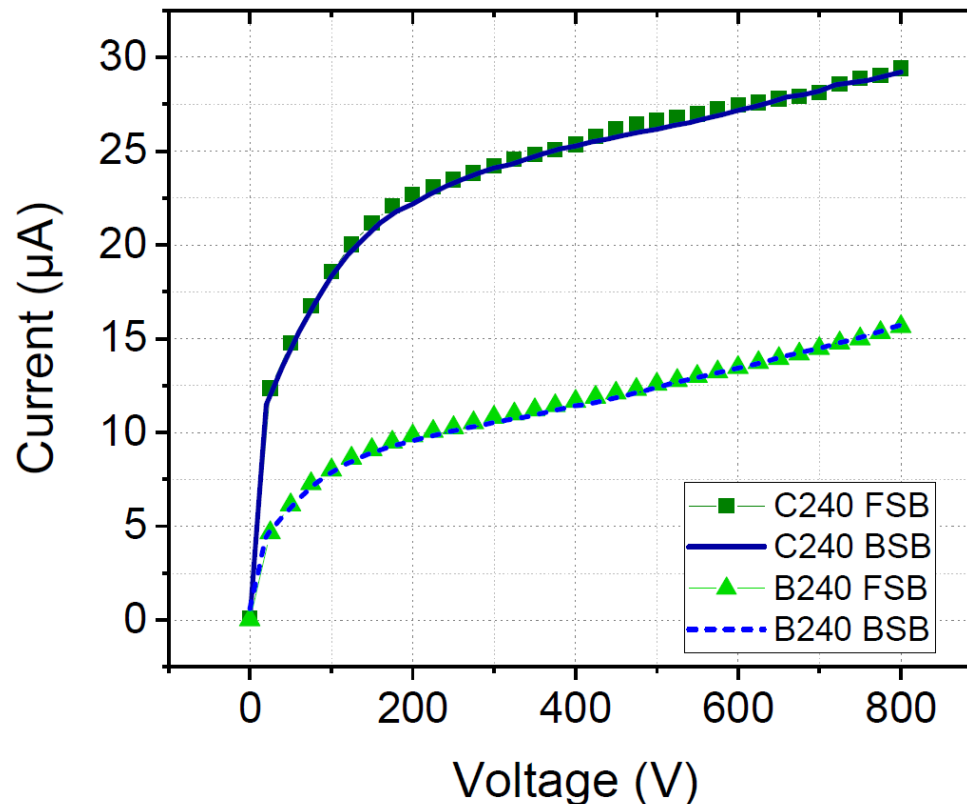
Sensor name	A_{sensor} (cm ²)	A_{edge} (cm ²)
A200	1.83	0.38
A240	1.83	0.38
B200	3.10	0.46
B240	3.10	0.46
C240	6.96	0.81
X240	96.66	2.54
D200*	13.49	1.01



*IFX, thinned

Example before irradiation

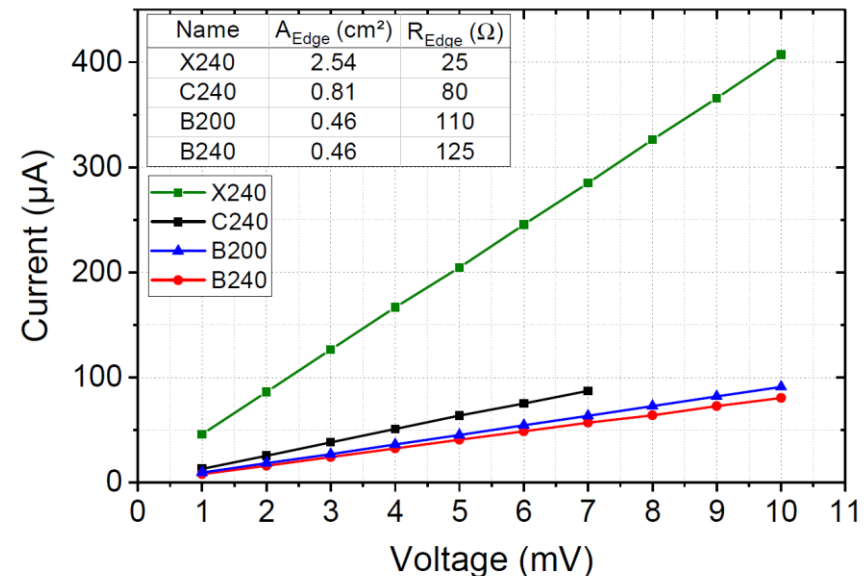
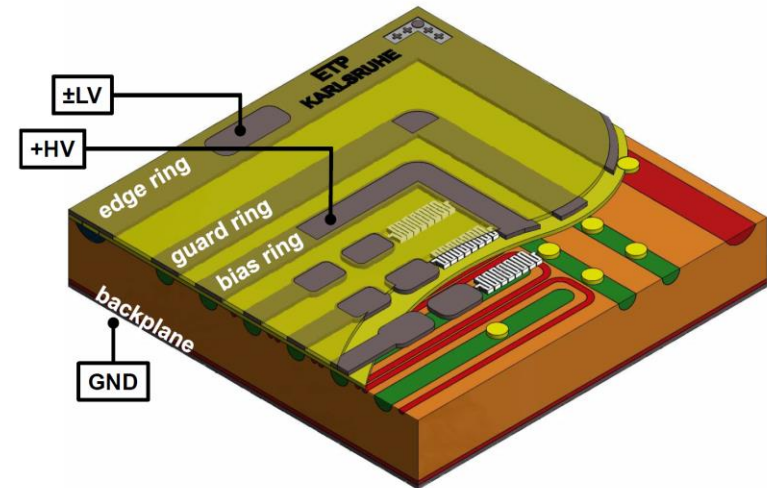
- Comparison of IV curves in FSB and BSB configuration can reveal voltage drops if they divert
 - typically they lie on top of each other



Edge resistivity

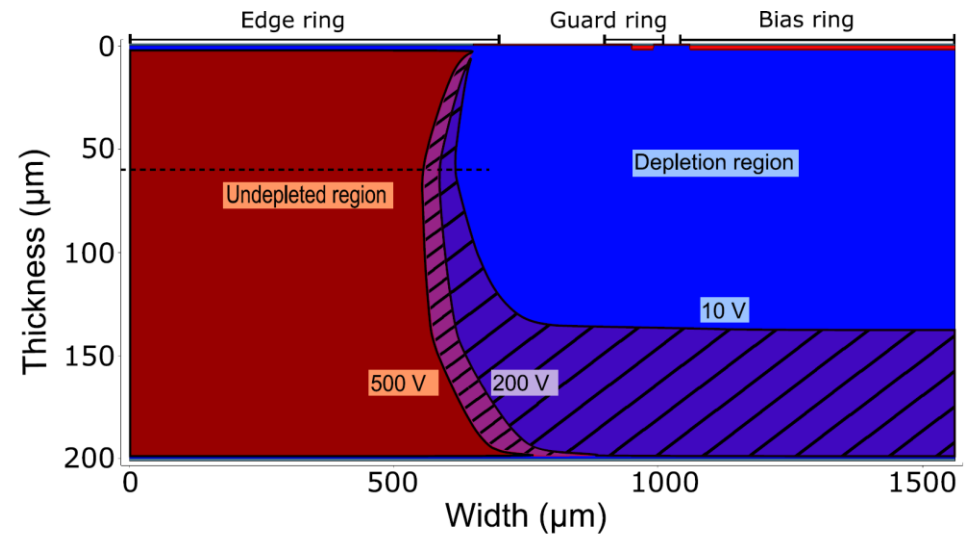
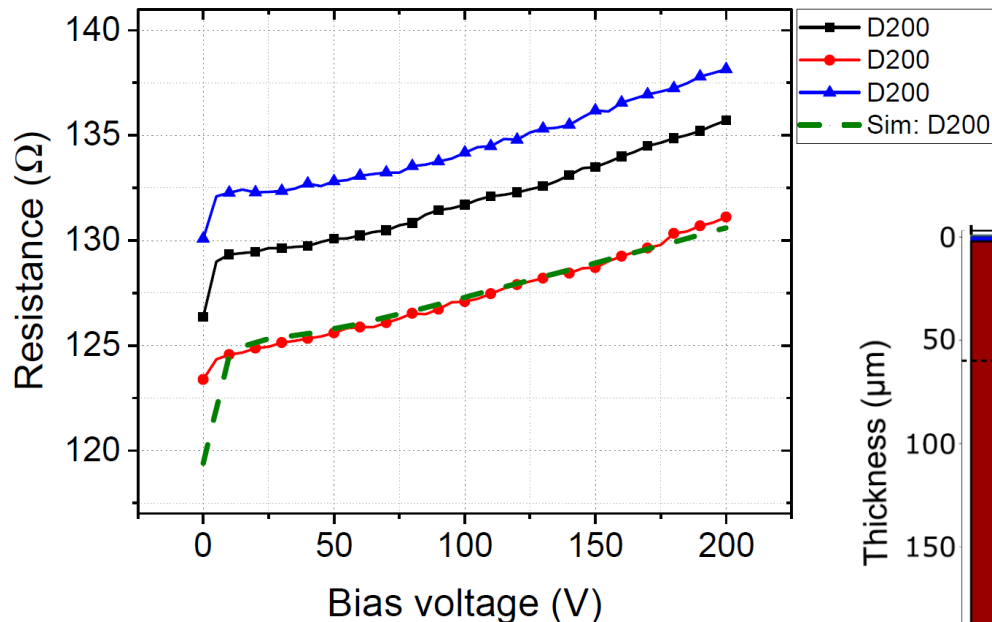
- The resistivity can be extracted by an IV curve over the edge, while the sensor is reverse biased
 - need to change potentials of applied bias on the probe station to get a common ground
- Edge resistivity and bulk resistivity are very similar

Material	ρ_{ER} (k Ω cm)	ρ_{CV} (k Ω cm)
240 μ m, ddFZ (HPK)	2.7 ± 0.2	3.0 ± 0.1
200 μ m, ddFZ (HPK)	2.6 ± 0.4	3.3 ± 0.1
200 μ m, FZ (IFX)	6.3 ± 0.6	6.5 ± 0.3



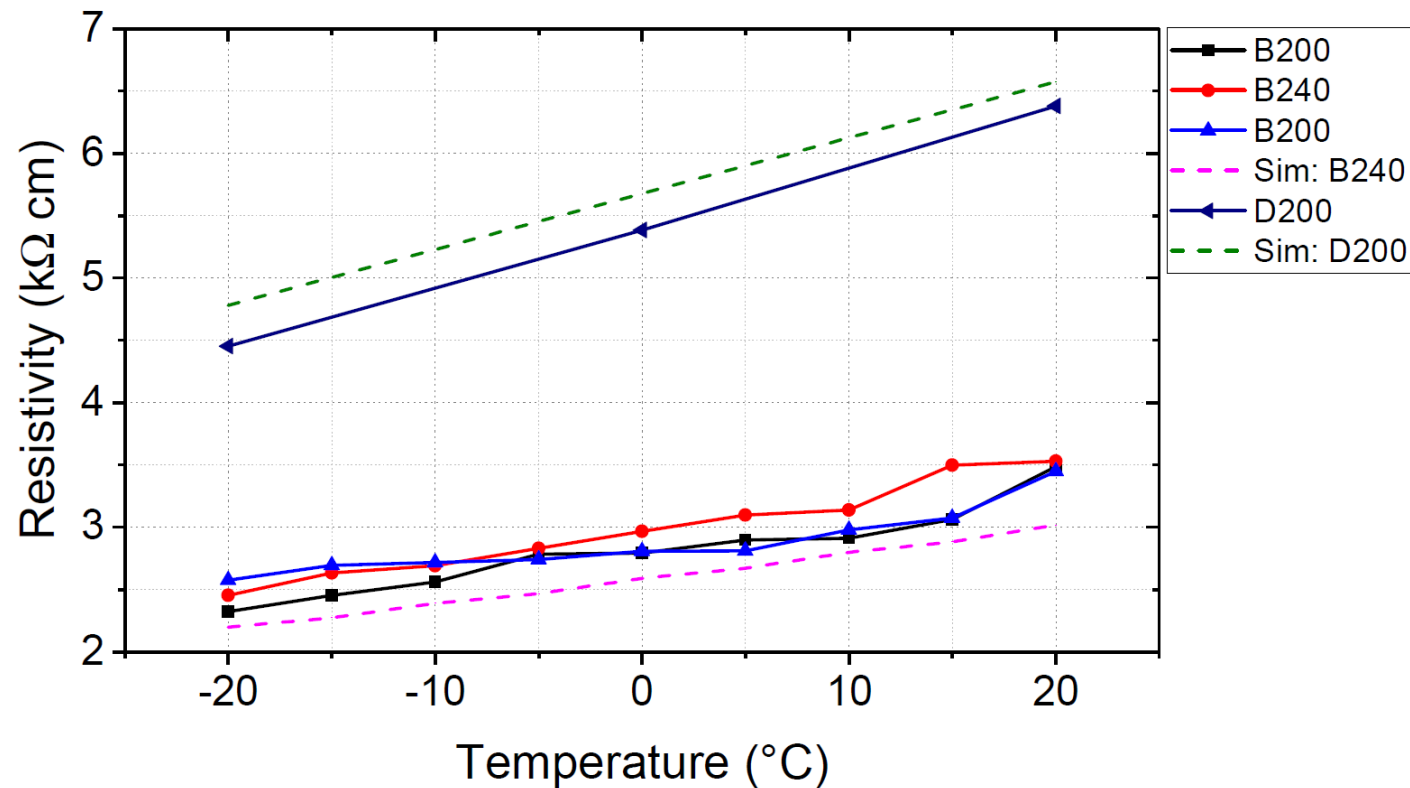
Bias voltage dependence

- Edge resistance increases with increasing bias and extending depletion zone
 - shrinkage of edge zone causes reduction of A_{edge}
 - increase supported by TCAD simulations



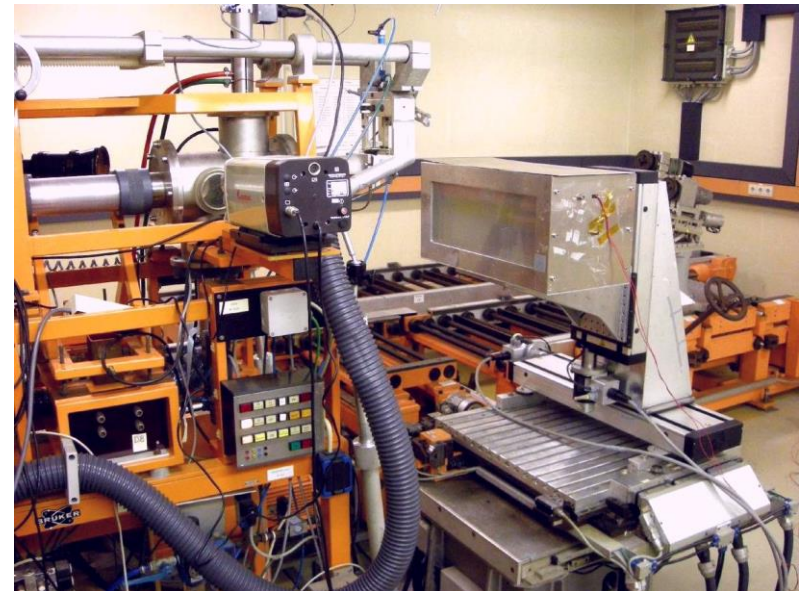
Temperature dependence

- The edge resistivity increases with increasing temperature
 - $\rho \sim T^{3/2}$ (phonon scattering)
 - increase supported by TCAD simulations



Irradiation

- 23MeV proton irradiation at KIT
- Fluences: $1 \times 10^{13} n_{eq}/cm^2$ to $2 \times 10^{15} n_{eq}/cm^2$
 - (dose: 15kGy – 3MGy)
- Performed cold (flushed with cold nitrogen gas of $\sim -30^\circ C$)
- Irradiating one sensor of 10mm x 20mm to $2 \times 10^{15} n_{eq}/cm^2$ takes about 20 minutes

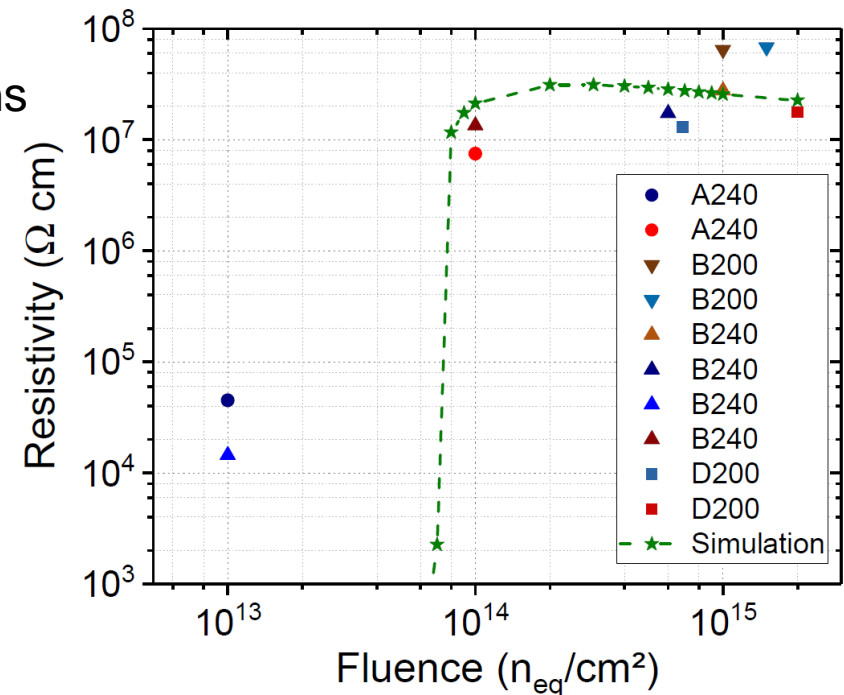


http://www.etp.kit.edu/english/irradiation_center.php

Resistivity vs. fluence

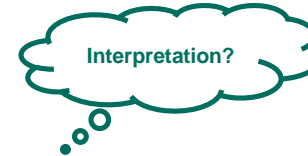
- We observe a severe increase of the edge resistivity with fluence
- At $1 \times 10^{14} n_{eq}/cm^2$ of 23MeV protons the edge resistivity reach $10 G\Omega cm$
- We also observe a kind of saturation
 - this is supported by TCAD simulations
- Extrapolation to large sensors:
 - 10cm x 10cm sensor
 - fluence $> 10^{14} n_{eq}/cm^2$
 - resistance to backplane: $\sim 150 k\Omega$
 - voltage drop: $\sim 150V$
 - unacceptable additional load on power system and cooling

→ no FSB at high fluence and large sensors

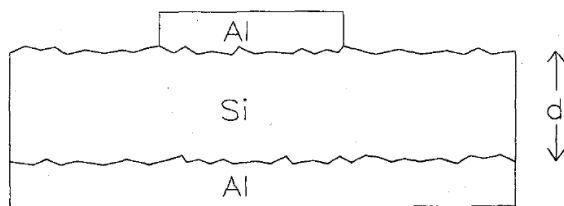


Extracted resistivity from edge resistivity measurements on irradiated mini sensors for different fluences at a temperature of $-20^\circ C$.

Influence of defects on resistivity



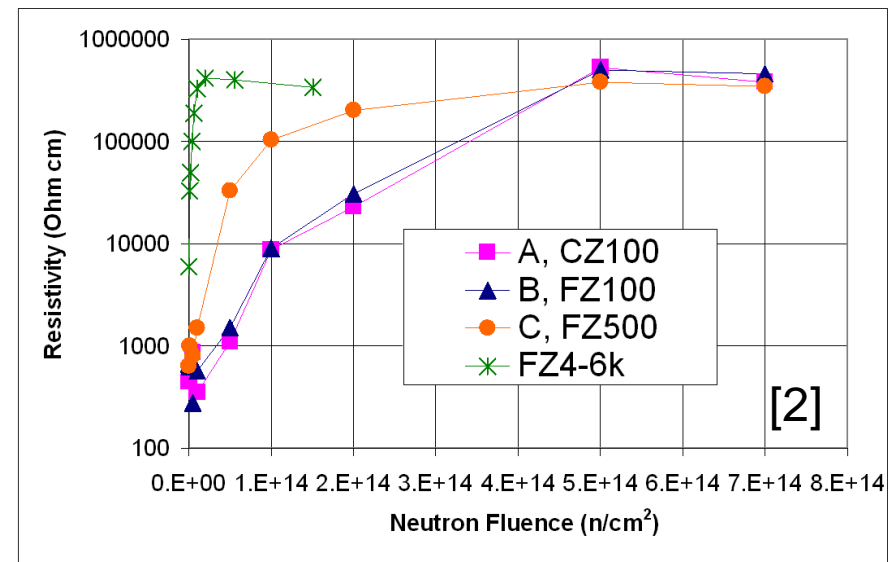
- The resistivity increases due to the process of “space charge limited currents” already known since long (e.g. [1])
 - Current through the edge is increased (bulk damage effect)
 - Large concentration of charge carriers in edge region occupy defects
 - Resulting E-field opposes current flow
 - Effective resistivity increases
- The fast increase of resistivity with fluence was also shown in [2]



IEEE Trans. Nucl. Sci. **46** (1999) 221.

[1] A. Taroni and G. Zanarini, “Space charge limited currents in P-N junctions”, *J. Phys. Chem. Solids* 30 (1969) 1861 – 1871.

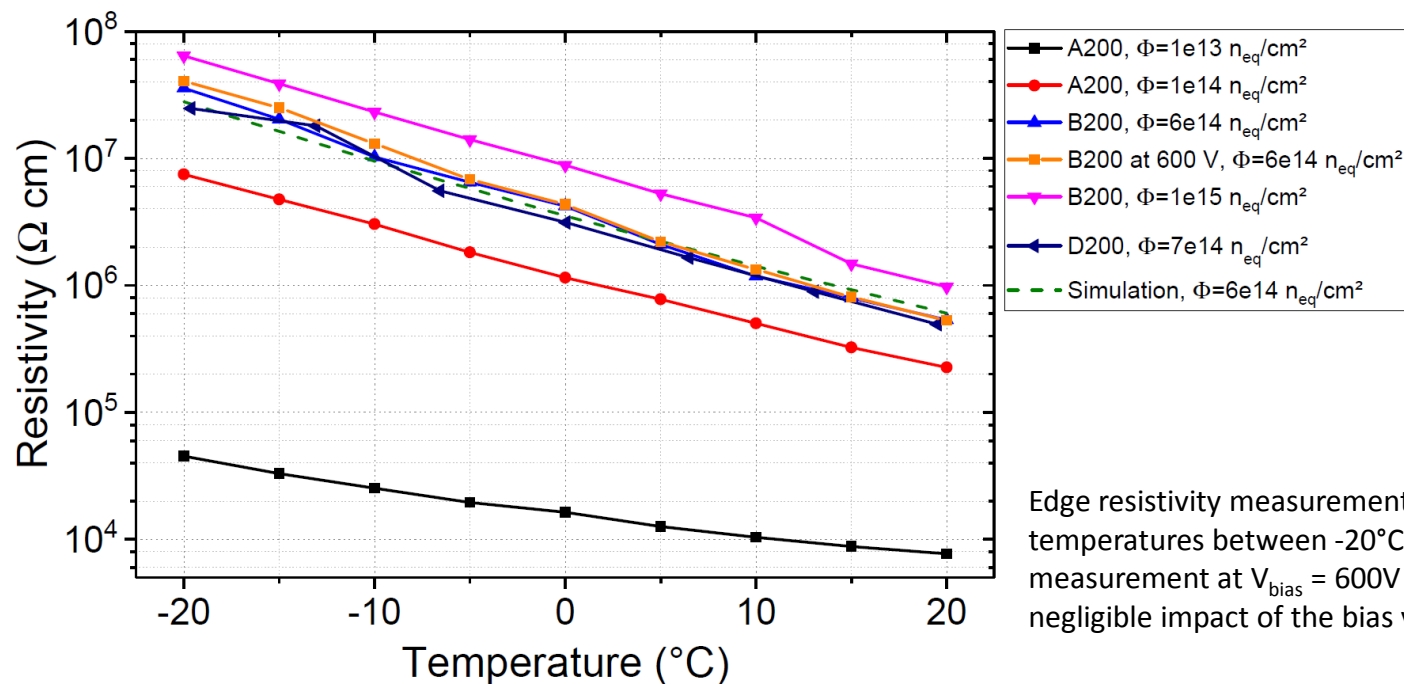
[2] Z. Li, “Radiation damage effects in Si materials and detectors and rad-hard Si detectors for SLHC”, *JINST* 4 (2009) P03011.



ENB resistivity, obtained from a direct resistor measurement, as a function of neutron fluence for n-type Si materials with different resistivity

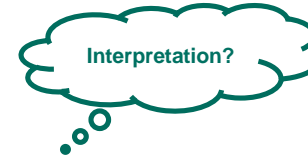
Resistivity vs. temperature (irrad.)

- After irradiation we also observe a reversed and more pronounced temperature dependence
 - non-irrad: ΔT of $-40^\circ\text{C} \rightarrow \rho \sim -40\%$
 - irrad.: ΔT of $-40^\circ\text{C} \rightarrow \rho$ from **+600%** to **+6600%**

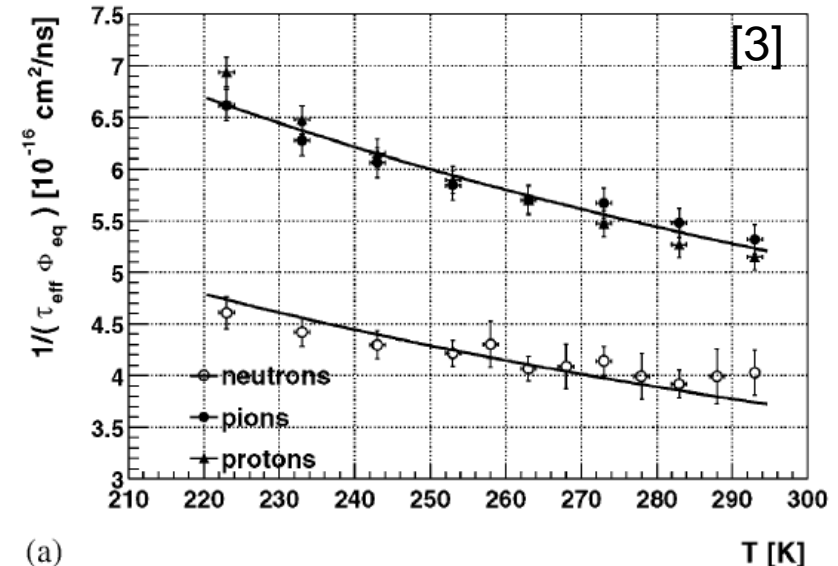


Edge resistivity measurements of irradiated sensors for temperatures between -20°C and $+20^\circ\text{C}$ at $V_{\text{bias}} = 0 \text{ V}$. A measurement at $V_{\text{bias}} = 600 \text{ V}$ was added to confirm the negligible impact of the bias voltage after irradiation.

Influence of trapping on resistivity



- Gregor showed in [3] that trapping probability decreases with increasing temperature
- Therefore less traps are occupied at higher temperature and resistivity is reduced
 - not clear if this explains the increase of resistivity to full extend...



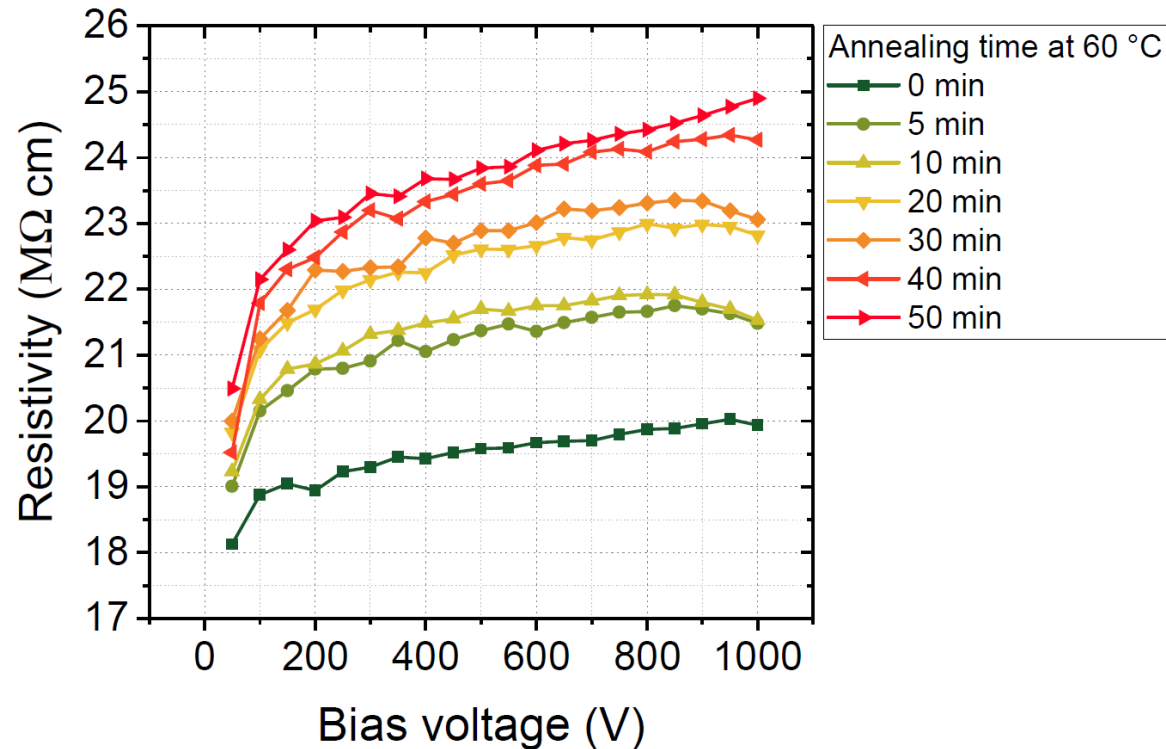
(a)

Fig. 3. Temperature dependence of β for: (a) electrons and (b) holes. The measured points are the average of β 's for all measured samples.

[3] G. Kramberger et al., "Effective trapping time of electrons and holes in different silicon materials irradiated with neutrons, protons and pions", *Nucl. Instr. and Meth.* 481 (2002) 297 – 305.

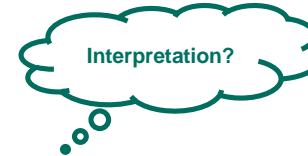
Resistivity vs. annealing

- Resistivity further increases with annealing



Measured resistivity of a D200 sensor irradiated to a fluence of $6.82 \times 10^{14} \text{ n}_{\text{eq}} \text{ cm}^{-2}$ with 23 MeV protons, as a function of the bias voltage and different annealing times.

Annealing of traps



- TCAD simulations were performed with varying trap concentrations
 - A decrease of the acceptor trap increases the resistivity at high fluence
- Several studies indicate that (at least) during beneficial annealing the defect concentration is reduced
 - Decrease of N_{eff} , i.e. shallow defects, was studied, but what about annealing of deeper defects responsible for trapping?
 - Deep acceptors like H(116K), H(140K), H(151K) would increase at least after beneficial annealing though...

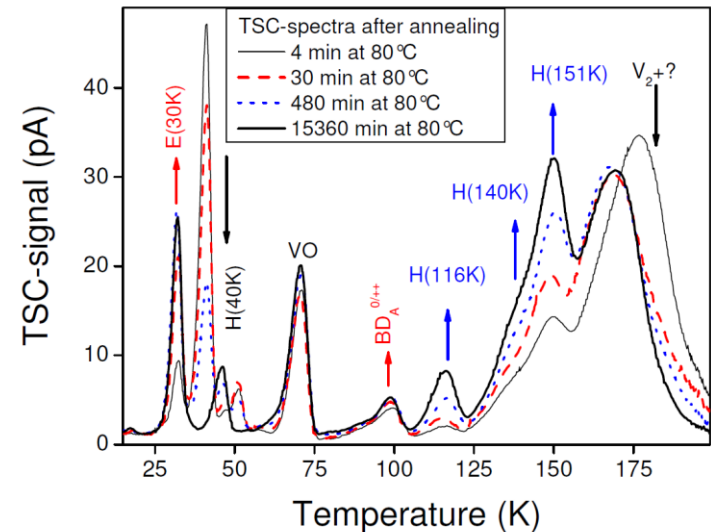
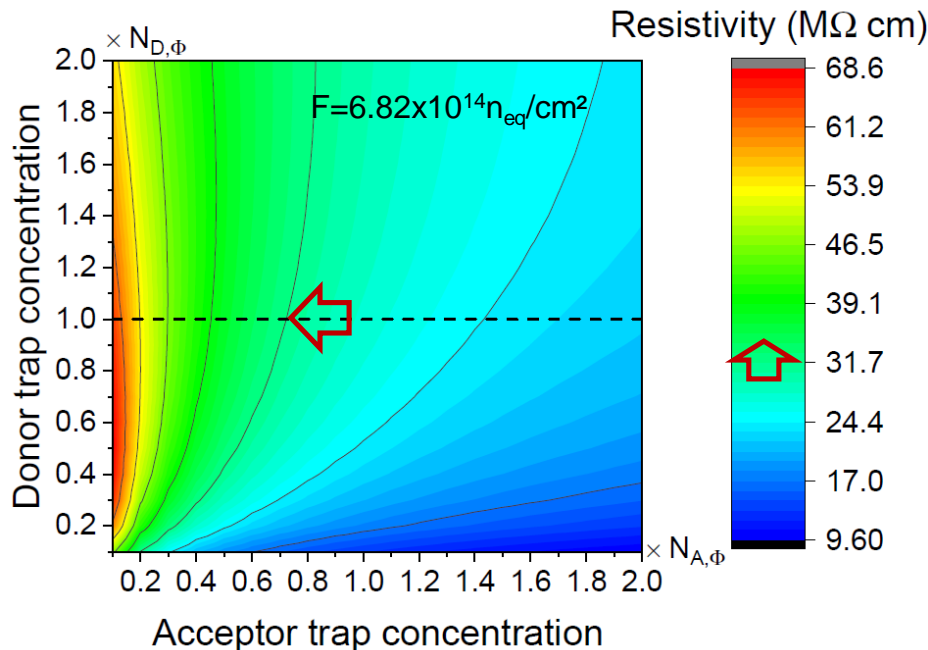
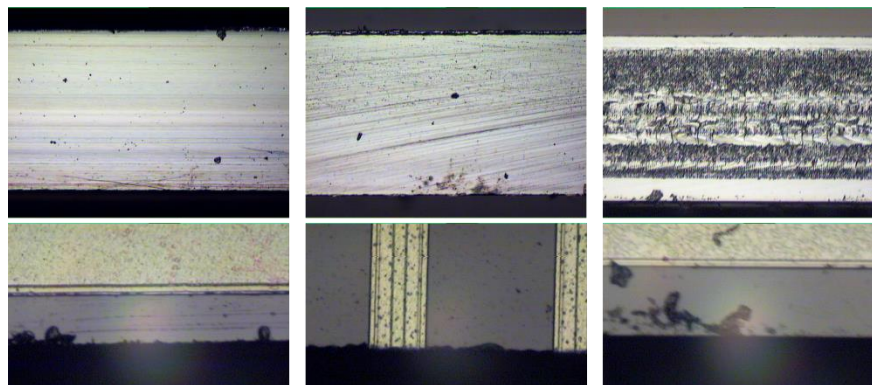


Figure 9.1.5: TSC spectra illustrating the shallow donors during annealing at 80 °C. Material: Epi-Do, fluence: $\Phi = 2 \times 10^{14} \text{ n cm}^{-2}$, measurement at $V_{\text{bias}} = 100 \text{ V}$.

A. Junkes, PhD, 2011

Intrinsic vs. practical case

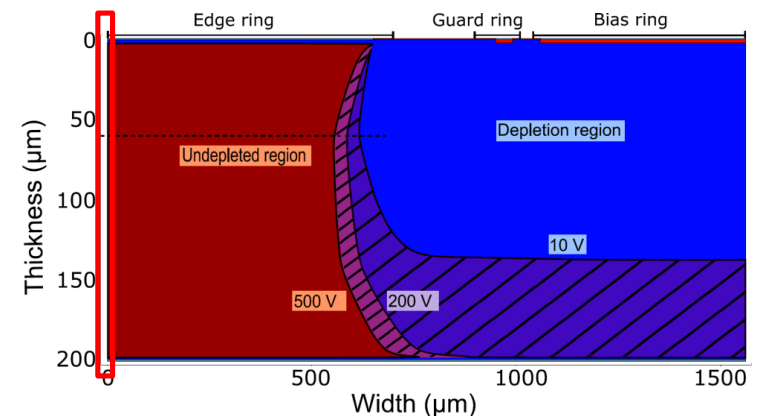
- These studies focused on the intrinsic properties of the silicon bulk
- In practice there could be severe distortions of the lattice at the diced edge
 - low ohmic path is possible at the cut edges
 - large scale detectors with long edge are more likely to be affected
 - not wise to rely mass production on such a mechanism
- Probability not too big since all mini-sensors in this study showed high resistance after irradiation without a short-circuit at the edge



Industrial saw

In-house saw

Laser dicing



Summary

- FSB would simplify module assembly in some cases
- Edge resistivity and dimensions influence parasitic bias resistance
- Very high edge resistivity starting from around $1 \times 10^{14} n_{eq}/cm^2$
 - not to be recommended for highly irradi. sensors with large leakage current
- Further findings:
 - Dependence of edge resistivity on T is reversed after irradiation
 - Resistivity further increases with short term annealing
- Further details in CMS NOTE-2018/002 and soon in JINST



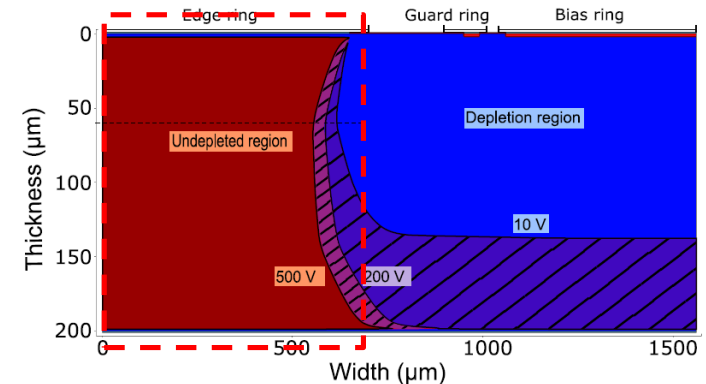
This project has received funding from the European Union's Horizon 2020 research and innovation programme under grant agreement No 654168



BACKUP

TCAD details

- Product: Synopsys Sentaurus
- Only oxide charge N_{ox} used; no interface traps or charge
- Simulated geometry: mainly the p^{++} - p - p^{++} region
- Physics models:
 - Fermi
 - Hydrodynamic(hTemperature)
 - Mobility (DopingDependence eHighFieldSaturation hHighFieldSaturation CarrierCarrierScattering (ConwellWeisskopf Enormal)
 - Recombination (SRH (DopingDependence TempDependence ElectricField (Lifetime=Hurkx DensityCorrection=none)) Auger eAvalanche (vanOverstraeten Eparallel) hAvalanche (vanOverstraeten Eparallel) Band2Band (Hurkx))
 - EffectiveIntrinsicDensity(Slotboom)
 - Recombination (CDL(TempDependence DopingDependence))
- Defect parameters:



Parameter	Donor	Acceptor
Energy (eV)	$E_V + 0.48$	$E_C - 0.525$
Conc. (cm^{-3})	$5.598 \text{ cm}^{-3} \times \Phi - 3.949 \cdot 10^{14}$	$1.189 \text{ cm}^{-3} \times \Phi + 6.454 \cdot 10^{13}$
$\sigma(e)$ (cm^2)	$1.0 \cdot 10^{-14}$	$1.0 \cdot 10^{-14}$
$\sigma(h)$ (cm^2)	$1.0 \cdot 10^{-14}$	$1.0 \cdot 10^{-14}$